Research Square

Preprints are preliminary reports that have not undergone peer review.
They should not be considered conclusive, used to inform clinical practice,
or referenced by the media as validated information.

Hydroxysafflor Yellow A Attenuates Microcirculatory Disturban ce in MAFLD via the EGFR/MAPK1 Pathway

Qing Liu
Heilongjiang University of Chinese Medicine
Nan Ai
Heilongjiang University of Chinese Medicine
Rui Wang
Heilongjiang University of Chinese Medicine
Zhenbo LI
Heilongjiang University of Chinese Medicine
Yihan Liu
Heilongjiang University of Chinese Medicine
Lei Wu
Heilongjiang University of Chinese Medicine
Yuqin Zhao
Heilongjiang University of Chinese Medicine
Jing Yang
yangjingdx@sina.com
Heilongjiang University of Chinese Medicine

Research Article

Keywords: Hydroxysafflor Yellow A, Metabolic Associated Fatty Liver Disease, Microcirculation Disturbance, EGFR/MAPK1 Signal Pathway

Posted Date: July 27th, 2026

DOI: https://doi.org/10.21203/rs.3.rs-10341374/v1

License: This work is licensed under a Creative Commons Attribution 4.0 International License.
Read Full License

Additional Declarations: No competing interests reported.

Version of Record: A version of this preprint was published at Naunyn-Schmiedeberg's Archives of Pharmacology on October 8th, 2026. See the published version at https://doi.org/10.1007/s00210-026-05980-9.

Hydroxysafflor Yellow A Attenuates Microcirculatory Disturbance in MAFLD via the EGFR/MAPK1 Pathway

Qing Liu[a],Nan Ai[a],Rui Wang[b,c],Zhenbo Li[b],Yihan Liu[b],Lei Wu[b],Yuqin Zhao[a],Jing Yang[a](corresponding author)
a College of Basic Medical Science, Heilongjiang University of Chinese Medicine, Harbin 150040, China
b College of Pharmacy, Heilongjiang University of Chinese Medicine, Harbin, 150040, China
c Key Laboratory of Basic and Application Research of Beiyao (Heilongjiang University of Chinese Medicine), Ministry of Education, Harbin 150040, China
Corresponding author：Jing Yang
E-mail address: yangjingdx@sina.com (Pro. Yang).Heilongjiang Univ Chinese Med, Coll Basic Med Sci, Harbin 150040, Peoples R China.

Abstract

The incidence of metabolic-associated fatty liver disease (MAFLD) continues to rise, making it a leading cause of chronic liver disease worldwide. Its pathological progression is frequently accompanied by microcirculatory dysfunction. However, effective therapeutic interventions targeting this specific process remain limited. Hydroxysafflor yellow A (HSYA) is the primary active component of Carthamus tinctorius L.. It exerts diverse pharmacological effects, including anti-inflammatory, antioxidant, and microcirculation-improving activities. However, the specific mechanisms by which HSYA regulates microcirculatory dysfunction in MAFLD have yet to be elucidated. In this study, a rat model of MAFLD was established using a methionine-choline deficient (MCD) diet to investigate the protective effects of HSYA and the underlying EGFR/MAPK1 signaling mechanism. The results showed that HSYA treatment significantly reduced serum levels of ALT, AST, TC, TG, and ET-1, while increasing NO levels. HSYA administration also expanded mesenteric microvascular diameter and accelerated blood flow velocity. Furthermore, HSYA alleviated hepatic steatosis and inflammatory injury. These effects were accompanied by the downregulation of EGFR, MAPK1, and VEGF expressions in the liver, thereby inhibiting the overactivation of the EGFR/MAPK1 pathway.In summary, HSYA effectively ameliorates hepatic injury and microcirculatory dysfunction in MAFLD rats. The underlying mechanism is associated with inhibiting the overactivation of the EGFR/MAPK1 signaling pathway and downregulating VEGF expression, which collectively restores the balance of microvascular structure and function. These findings provide

experimental evidence for the therapeutic potential of HSYA in treating MAFLD-related microcirculatory disorders.
Keywords:Hydroxysafflor Yellow A; Metabolic Associated Fatty Liver Disease; Microcirculation Disturbance; EGFR/MAPK1 Signal Pathway;

1.Introduction

Metabolic-associated fatty liver disease (MAFLD), formerly known as non-alcoholic fatty liver disease (NAFLD), is a chronic liver injury disorder driven by multisystemic metabolic dysfunction. Its disease spectrum encompasses simple fatty liver, non-alcoholic steatohepatitis (NASH), hepatic fibrosis, cirrhosis, and hepatocellular carcinoma [1]. According to the 2025 APASL Clinical Practice Guidelines, the prevalence of MAFLD in the Asia-Pacific region ranges from 28% to 40%, ranking it among the highest globally. Specifically, the prevalence rates are 34% in South Asia, 33% in Southeast Asia, and 30% in East Asia. This represents a significant increase compared to the 29.62% reported in the 2020 guidelines [2]. A clinical study involving 22,970 patients in China reported an MAFLD prevalence of 28.77% among the urban population. Notably, approximately 16.87% of these patients exhibit significant hepatic fibrosis [3].

The onset and progression of MAFLD are closely linked to disorders of lipid metabolism and insulin resistance. Under physiological conditions, insulin inhibits hepatic gluconeogenesis and promotes the synthesis of lipids. Research by Professor Jiajun Zhao's team revealed that hepatic lipid deposition is primarily driven by three synergistic pathways: enhanced adipose tissue lipolysis, impaired skeletal muscle glucose metabolism, and abnormal activation of hepatic lipid synthesis pathways. These processes lead to a massive influx of free fatty acids (FFAs) and glucose into the liver, promoting lipid synthesis and accumulation, which ultimately induces MAFLD [4]. The inflammatory response is a critical factor in MASLD progression. Inflammation exacerbates hepatic tissue injury through leukocyte infiltration and the release of proinflammatory cytokines. Furthermore, it can induce hepatocyte apoptosis, insulin resistance, and lipid metabolism disorders in the liver. These processes subsequently drive the transition from MAFLD to non-alcoholic steatohepatitis (MASH) and potentially to cirrhosis and hepatocellular carcinoma [5]. Research has indicated that inhibiting the inflammatory response can ameliorate MAFLD. The underlying mechanisms involve reducing intrahepatic lipid content, enhancing fatty acid β-oxidation, activating hepatoprotective autophagy, and improving insulin sensitivity[6]. Elevated levels of hepatic reactive oxygen species (ROS) are a significant factor in the onset and progression of MAFLD. Excessive ROS not only directly damage intracellular structures, leading to hepatocyte injury and apoptosis, but also interfere with insulin signaling and innate immune responses, thereby disrupting lipid metabolism homeostasis[7]. Additionally, research has identified the gut microbiota as a key player in MAFLD pathogenesis via the "gut-liver axis," primarily influencing hepatic metabolism, immunity, and inflammatory status. Gut dysbiosis can compromise the integrity of the intestinal barrier, facilitating the entry

of gut-derived toxins such as lipopolysaccharides (LPS) into the portal venous system. This process activates hepatic inflammatory responses and promotes lipid deposition[8].

As MAFLD progresses, pathological changes occur in multiple components of the hepatic microcirculatory system, leading to microcirculatory dysfunction. This dysfunction triggers various pathological mechanisms, including exacerbated insulin resistance, endothelial dysfunction, elevated oxidative stress, and abnormal lipid metabolism. These factors eventually interact with systemic metabolic disorders, establishing a vicious cycle that drives disease progression.In the regulation of microcirculatory blood flow, beyond vascular smooth muscle cells, liver sinusoidal endothelial cells (LSECs), hepatic stellate cells (HSCs), and Kupffer cells (KCs) collectively participate in the regulatory mechanism[9]. During the simple steatosis stage of MAFLD, LSECs undergo significant phenotypic shifts characterized by the loss of fenestrae and the development of a subendothelial basement membrane—a process termed “capillarization.” [10]. This structural remodeling impairs the bidirectional exchange between sinusoids and hepatocytes, leading to cellular hypoxia, apoptosis, and necrosis. Consequently, the release of damage-associated molecular patterns (DAMPs) is triggered, fueling the progression of hepatic inflammation[11]. DAMPs and various cytokines secreted by LSECs can activate HSCs, inducing their transformation into a myofibroblast-like phenotype. This activation leads to excessive synthesis and secretion of extracellular matrix (ECM), which ultimately drives the progression of hepatic fibrosis[12]. HSCs are non-parenchymal liver cells located in the perisinusoidal space (space of Disse). During MAFLD progression, HSCs are activated by pathological stimuli, such as inflammatory cytokines and oxidative stress[13]. This activation triggers a phenotypic transition into myofibroblast-like cells, characterized by the loss of lipid droplets and the synthesis of abundant extracellular matrix components, including collagen types I and III. These processes induce hepatic fibrosis, leading to sinusoidal remodeling and increased resistance to blood flow. Consequently, the stability of the hepatic microcirculation is disrupted, exacerbating tissue hypoxia and liver dysfunction[14]. KCs are resident hepatic macrophages, and their functional imbalance is a critical link between microcirculatory dysfunction and immunoinflammatory dysregulation. During MAFLD progression, KCs polarize into M1 or M2 phenotypes to mediate inflammatory responses. Specifically, M1-type cells release cytokines, such as IL-1β and TNF-α, via pathways including TLR4/NF-κB and JAK/STAT1. This exacerbates intrahepatic inflammation and vascular endothelial injury, disrupting microcirculatory stability. Conversely, M2-type cells secrete mediators such as IL-10 and TGF-β through pathways such as JAK/STAT6 and TGFβ/Smads, promoting tissue repair and angiogenesis[15]. These cytokines further damage LSECs and induce HSC activation, establishing a vicious cycle of “inflammation-microcirculatory dysfunction-fibrosis”[16]. Local pathological changes resulting from hepatic microcirculatory dysfunction, such as sinusoidal capillarization, sinusoidal narrowing, portal hypertension, and abnormal angiogenesis, not only exacerbate the

progression of MAFLD but also impact systemic vascular endothelial function and microcirculatory homeostasis through mechanisms including inflammation, endothelial dysfunction, and insulin resistance[17]. Peripheral microcirculation in MAFLD patients exhibits a hemodynamic disorder characterized by reduced microvascular perfusion and impaired endothelium-dependent vasoreactivity. The specific mechanisms are shown in Figure 1.

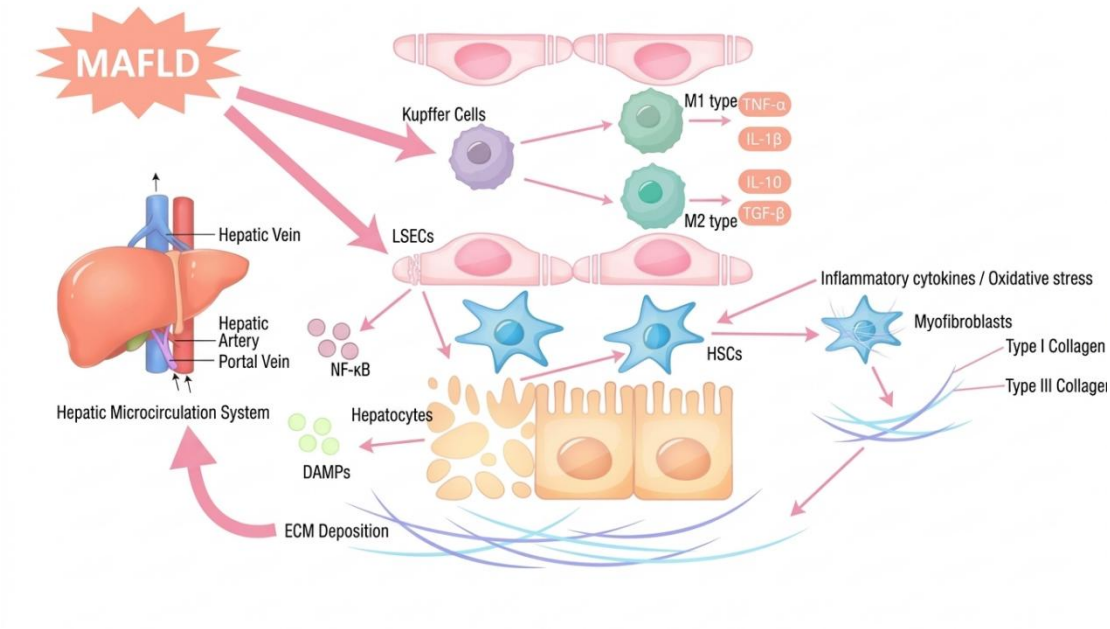


Figure 1.Mechanisms underlying the association between metabolic-associated fatty liver disease (MAFLD) and microcirculatory dysfunction.

As the primary active constituent of Carthamus tinctorius L., HSYA exerts protective effects against liver injury induced by various etiologies by modulating multiple signaling pathways and targeting various molecular targets. Its underlying mechanisms involve multidimensional biological effects, including anti-inflammatory, antioxidant, and anti-fibrotic activities, and the regulation of hepatic metabolism[18].To the best of our knowledge, no study has demonstrated the protective effects of HSYA against microcirculatory dysfunction in MAFLD rats. Therefore,the purpose of this investigation was to assess the preventive effects of HSYA on microcirculatory dysfunction in a rat model of MAFLD and to ascertain whether the EGFR/MAPK1/VEGF pathway is implicated. The results offer the first experimental proof that HSYA is a viable treatment option for microcirculatory dysfunction linked to MAFLD.

2.Materials and Methods

2.1 Animal Model and Drugs Administration

The Male Sprague-Dawley (SD) rats (6–8 weeks old, weighing 200 ± 20 g) were purchased from the Safety and Drug Evaluation Center of the Heilongjiang University of Chinese Medicine (Heilongjiang, China). The animal production license number was SCXK (Liao) 2020-0001. All rats were housed in a st

andard environment with a 12 h light/dark cycle, controlled temperature (20–25 °C), and relative humidity (50%–65%). The animals were given free access to food and water and acclimated for one week before the experiment.

After one week of acclimation, the rats were randomly divided into 6 gro ups (n=6 per group): control group (CON, normal diet), model group (MOD, MCD diet), positive control group (PC, MCD diet + silibinin 20 mg/kg/d)[19]. [20], HSYA low-dose group (HSYA-L, MCD diet + HSYA 7.5 mg/kg/d), HSY A middle-dose group (HSYA-M, MCD diet + HSYA 15 mg/kg/d), and HSYA high-dose group (HSYA-H, MCD diet + HSYA 30 mg/kg/d)[21]. The MCD die t was administered for 8 weeks, and drug interventions were administered by i ntraperitoneal injection once daily during the last 4 weeks.

2.2 General Observation of Experimental Rats

During the experimental period, the general status of the animals in each group was observed and recorded. This assessment included food and water int ake, luster of fur and claws, mental activity levels, and behavioral responsivene ss. In addition, fecal and urinary characteristics and mortality rates were monit ored. The body weight of the experimental animals was systematically measure d and documented on a weekly basis to monitor growth trends.

2.3 Histopathological Observation of Liver Tissue

Following the administration period, liver tissue samples were harvested an d preserved in a 4% paraformaldehyde solution for a duration of 24 hours. Th e samples were then dehydrated using a graded series of ethanol, embedded in paraffin, and sectioned into 4-μm thick slices using a microtome. Finally, the sections were stained with hematoxylin and eosin (H&E) and sealed for histolo gical examinations.

2.4 Biochemical Analysis

An enzyme-linked immunosorbent assay (ELISA) was employed to detect t he levels of hepatic function indicators (ALT and AST), lipid metabolism para meters (TC and TG), and microcirculatory dysfunction markers (NO and ET-1) in each group. Serum samples stored at -20°C were thawed at room temperat ure (20–25°C). In accordance with the manufacturer's instructions, samples were introduced into the microplate wells for detection purposes. These measuremen ts were used to evaluate the extent of liver injury, lipid metabolism disorders, and changes in microcirculatory function during MAFLD progression.

2.5 Detection of Mesenteric Microcirculation

After anesthesia, the rats were placed in a supine position and secured to the surgical platform. A midline abdominal incision was made to expose the p eritoneal cavity, and a segment of the mesentery was gently exteriorized and pl aced in a constant-temperature water bath. The light source of the mesenteric microcirculation detector was activated, and the focal length was adjusted. Suita ble mesenteric microvessels were selected for observation under a microscope. Once the physiological state of the rats was stabilized, the microcirculatory dyn amics of the target vessels within the same field of view were continuously m onitored and recorded. Key hemodynamic parameters, such as Arteriolar diamet

er (DA), Venule diamater (DV), the DA/DV ratio, blood flow velocity area (BFVA), and blood flow velocity volume (BFVV), were systematically analyzed. Additionally, the patterns of blood flow, including linear and granular flow, were documented. All measurements were conducted under identical conditions of illumination, temperature (37°C), and field of view. To minimize individual variation and experimental error, each rat was tested three times, and the mean values were calculated to objectively reflect the degree of microcirculatory dysfunction in the MAFLD models and the therapeutic efficacy of HSYA.

2.6 RT-qPCR Analysis

Total RNA was extracted from rat liver tissues and reverse-transcribed into complementary DNA (cDNA). Subsequently, real-time quantitative PCR (RT-qPCR) was performed using the SYBR Green method to detect the mRNA transcription levels of the target genes, including EGFR, MAPK1 (ERK2), and VEGF. β-actin was used as the internal control, and relative gene expression levels were calculated using the 2-△△CT method.

2.7 Western Blotting Analysis

Total protein was extracted from the liver tissues, and the concentrations were determined using the BCA assay. The protein samples were separated by SDS-PAGE and transferred onto PVDF membranes. After blocking with 5% non-fat milk, the membranes were incubated overnight at 4°C with primary antibodies (p-EGFR, EGFR, p-MAPK1, MAPK1, and VEGF). On the following day, the membranes were incubated with HRP-conjugated secondary antibodies at room temperature. The protein bands were visualized using the enhanced chemiluminescence (ECL) method, and the gray values of the bands were quantified using the ImageJ software. The ratios of phosphorylated proteins to their corresponding total proteins were calculated.

2.8 Immunohistochemical Analysis

Paraffin-embedded liver sections were deparaffinized, rehydrated, and subjected to antigen retrieval. After blocking endogenous peroxidase activity with 3% H2O2 and serum blocking, the sections were incubated with a primary antibody against VEGF overnight at 4°C. The signal was developed using the streptavidin-peroxidase (SP) method, followed by hematoxylin counterstaining. After dehydration, clearing, and mounting, the sections were observed and photographed using an optical microscope. For semi-quantitative analysis, five randomly selected non-overlapping fields per section at 200× magnification were captured from each animal. Three sections per rat, spaced at least 50 μm apart, were analyzed. The mean optical density (MOD) of VEGF-positive staining (brown precipitate) was measured using ImagePro Plus software with a fixed threshold applied uniformly to all images. All image acquisition and quantification were performed by an investigator blinded to the experimental groups. The MOD values from the five fields were averaged to obtain a single value per section, and the three section values were then averaged for each animal. The MOD was used to evaluate the intensity of VEGF expression in the liver tissue.

2.9 Data Analysis

Statistical analyses were performed using GraphPad Prism 9.0 and SPSS version 27.0. Quantitative data are expressed as mean ± standard deviation (SD). Comparisons among multiple groups were performed using one-way analysis of variance (ANOVA), followed by Tukey's post-hoc test for pairwise comparisons. Statistical significance was set at $p < 0.05$, and highly significant at $P < 0.01$. To ensure precision, quantitative data were reported to two decimal places, whereas ratios were reported to three decimal places.

3.Results

3.1 Effect of HSYA on growth and development

Compared with the control group, rats in the model group exhibited lethargy, reduced physical activity, coarse and lackluster fur, decreased food intake, loose stools, and a significant reduction in body weight ($P < 0.01$). After 4 weeks of HSYA intervention, the overall condition of the rats in each treatment group improved markedly, characterized by smoother and shinier fur, increased activity, and restored appetite. As shown in Figure 2, the body weights of all MAFLD model rats were significantly lower than those of the blank control group before drug administration ($P < 0.01$). After 4 weeks of treatment, the body weight of the model group continued to decline ($P < 0.01$). In contrast, body weight was significantly increased in the positive control (silibinin) and medium- and high-dose HSYA groups compared to the model group ($P < 0.01$), and a significant increase was also observed in the low-dose HSYA group ($P < 0.05$). These results demonstrate that HSYA exerts a dose-dependent ameliorative effect on body weight loss in MAFLD-model rats.

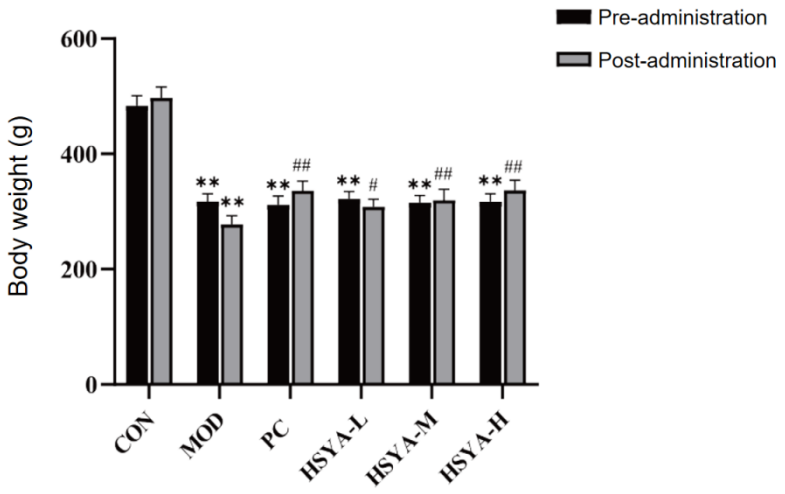


Figure 2. Effect of HSYA on body weight in MAFLD rats. Body weight was recorded before and after 4 weeks of treatment. Data are presented as mean ± SD (n = 6). $^{**}P < 0.01$ vs. Blank Control group; $^{\#}P < 0.05$, $^{\#\#}P < 0.01$ vs. Model group.

3.2 Effects of HSYA on hepatic histopathology in rats

As shown in Figure 3, the liver tissue in the blank control group displayed

a complete structural architecture with clearly defined and well-ordered hepatic cords, regular hepatocyte morphology, and centrally located round nuclei. In contrast, the MAFLD model group exhibited significant structural damage, characterized by numerous lipid vacuoles (fatty vacuoles), disrupted hepatic lobular architecture, disordered hepatic cords, and inflammatory cell infiltration, confirming successful establishment of the MAFLD model. Compared to the model group, HSYA intervention resulted in varying degrees of improvement in hepatic pathological injury. The reduction of lipid droplets within hepatocytes was most notable in the positive control group, as well as in the medium- and high-dose HSYA groups. In these groups, the arrangement of hepatic cords was more orderly, the hepatic lobular structure was partially restored, and the nuclei were clearly visible.

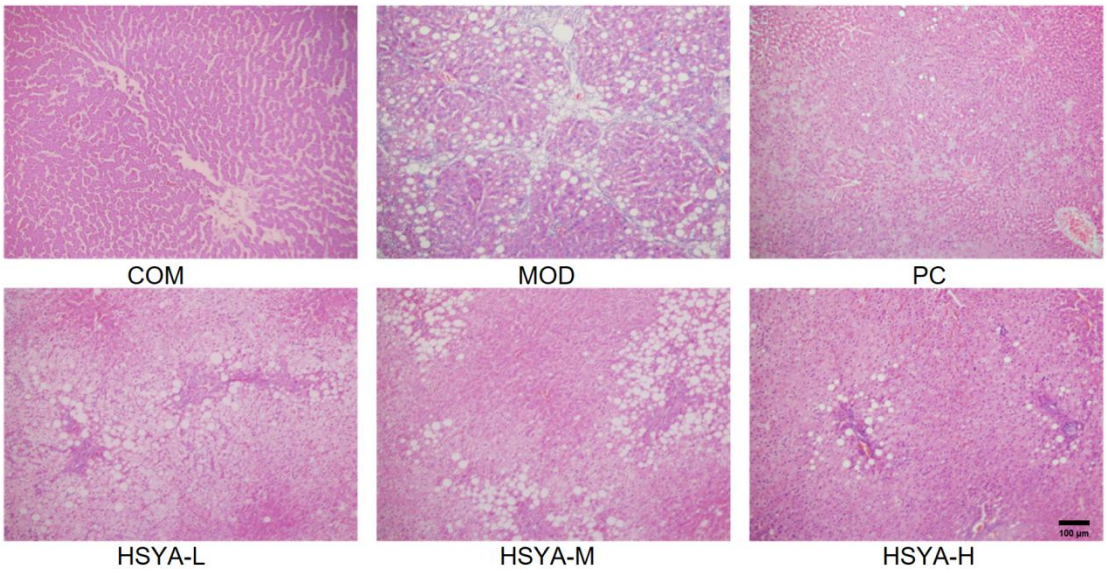


Figure 3. Effects of HSYA on hepatic histopathology in MAFLD rats (HE staining×100).

3.3. Effects of HSYA on serum biochemical parameters in rats

Compared with the control group, the serum levels of ALT, AST, TC, and TG were significantly elevated in the model group ($P < 0.01$), indicating severe liver injury and lipid metabolism disorders. The administration of HSYA resulted in a dose-dependent decrease in the levels of ALT, AST, TC, and TG ($P<0.05$，$P<0.01$), suggesting that HSYA intervention effectively mitigates hepatic functional impairment and lipid metabolic abnormalities. Meanwhile, serum NO levels significantly decreased and ET-1 levels significantly increased in the model group ($P<0.05$，$P<0.01$). HSYA treatment significantly increased NO levels and decreased ET-1 levels ($P<0.05$，$P<0.01$), indicating that HSYA improves endothelial vascular dysfunction by regulating the levels of vascular endothelial-related factors(Figure 4A–F).

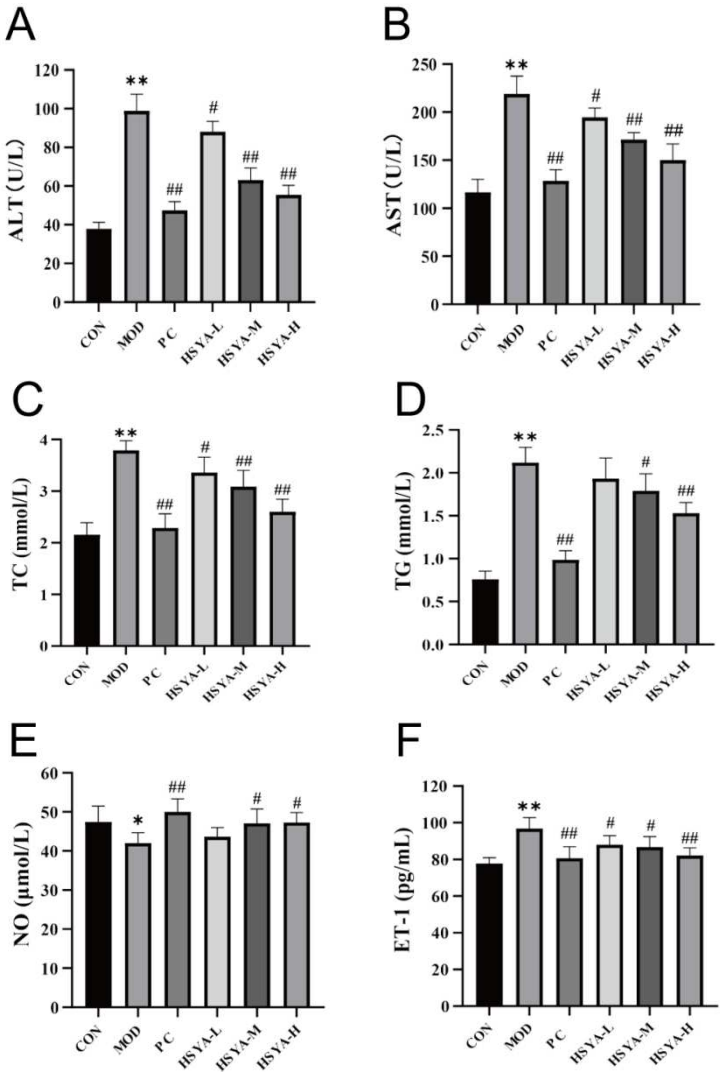


Figure 4. Effects of HSYA on serum biochemical in MAFLD rats. (A) ALT, (B) AST, (C) TC, (D) TG, (E) NO and (F) ET-1. Data are presented as mean ± SD (n = 6). $^{**}P < 0.01$ vs. Blank Control group; $^{\#}P < 0.05$, $^{\#\#}P < 0.01$ vs. Model group.

3.4. Effects of HSYA on mesenteric microcirculation in MAFLD rats

The results shown in Figure 5 demonstrate that the mesenteric microvessels in the blank control group exhibited regular morphology with smooth and even vessel walls, and the blood flow was predominantly linear or line-granular, indicating satisfactory perfusion. In contrast, the mesenteric microvessels in the MAFLD model group showed disordered structures and tortuous paths, with overall poor blood flow. The blood flow patterns identified in this cohort were primarily granular or granular-linear, with numerous interruptions. Compared with the model group, HSYA intervention at various doses and the positive control led to varying degrees of improvement in microvascular filling and enhanced blood flow. The blood flow patterns gradually shifted back toward linear and granular flows. Notably, the positive control and high-dose HSYA groups exhibited the most significant improvements.

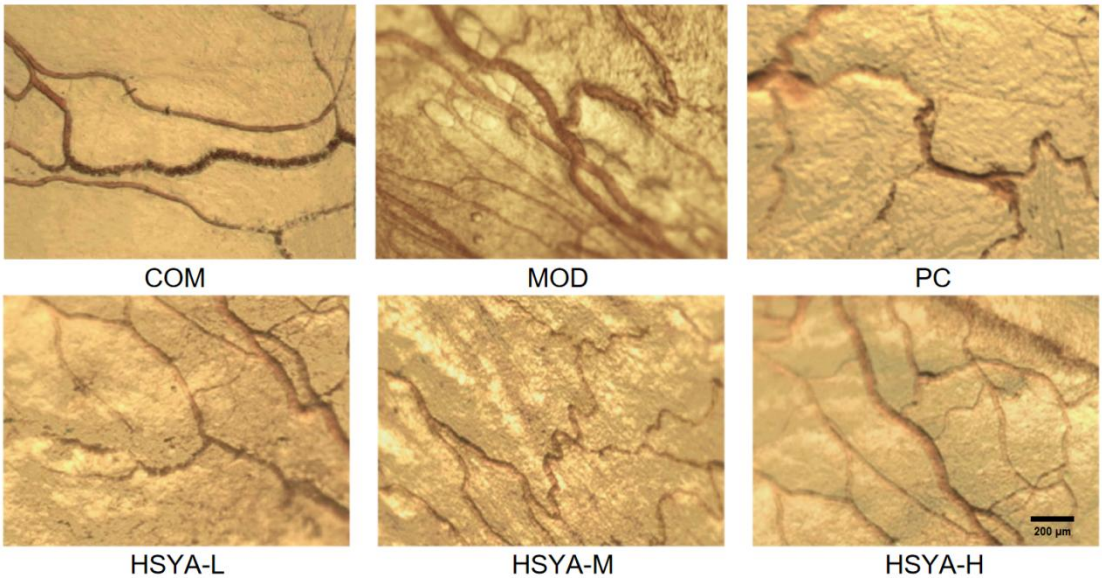


Figure 5. Effects of HSYA on mesenteric microcirculation in MAFLD rats. Representative photomicrographs of mesenteric microvessels(×200)

As shown in Table 1 and Figure 6, compared with the blank control group, the mesenteric arteriolar diameter (DA) was significantly decreased, venular diameter (DV) was significantly increased, and DA/DV ratio was markedly reduced in the MAFLD model group ($P < 0.01$, $P < 0.05$). These findings indicate an arteriovenous diameter imbalance and microcirculatory dysfunction in the model group rats.After 4 weeks of intervention, compared with the model group, the positive control group showed a significant increase in DA ($P < 0.01$), a downward trend in DV, and a significant increase in the DA/DV ratio ($P < 0.01$). All HSYA-treated groups exhibited varying degrees of improvement in their health. Among them, the high-dose HSYA group showed the most pronounced therapeutic effect, with a significant increase in DA ($P < 0.05$) and a significant elevation in the DA/DV ratio ($P < 0.01$). These results suggest that HSYA treatment effectively corrects arteriovenous diameter imbalance and facilitates venous return, thereby improving microcirculatory function in MAFLD rats.

Table 1. Effects of HSYA on DA, DV, and DA/DV ratio in mesenteric microvessels of rats

Groups	**DA(μm)**	**DV(μm)**	**DA/DV**
CON	25.09±3.04	29.70±2.69	0.84±0.04
MOD	20.35±3.41*	32.70±1.14*	0.63±0.12**
PC	25.44±2.88$^{\#\#}$	30.87±1.65	0.82±0.08$^{\#\#}$
HSYA-L	22.28±1.67	31.92±3.41	0.70±0.03
HSYA-M	23.43±2.23	31.87±1.99	0.73±0.04
HSYA-H	24.77±1.98$^{\#}$	31.70±2.22	0.78±0.08$^{\#\#}$

Note: Data are expressed as mean ± SD (n = 6). $^{**}P < 0.01$ vs. Blank Control group; $^{\#}P < 0.05$, $^{\#\#}P < 0.01$ vs. Model group.

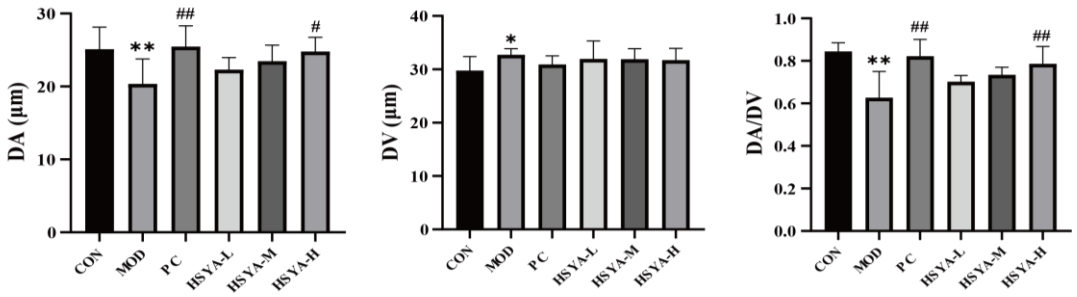


Figure 6. Effects of HSYA on mesenteric microvascular morphology in MAFLD rats. The mesenteric microvascular DA (left) and DV (center) were measured, and the DA/DV ratio (right) was calculated. Data are presented as mean ± SD (n = 6). $^{**}P < 0.01$ vs. Blank Control group; $^{\#}P < 0.05$, $^{\#\#}P < 0.01$ vs. Model group.

As shown in Table 2 and Figure 7, compared with the control group, both BFVA and BFVV in the mesenteric microvasculature of rats in the model group were significantly reduced ($P < 0.01$), suggesting a decline in microvascular perfusion capacity and an impaired microcirculatory function. After 4 weeks of drug intervention, compared with the model group, both BFVA and BFVV in the positive drug group were significantly increased ($P < 0.01$), approaching the levels of the control group. All dose groups of HSYA improved microvascular blood flow to varying degrees. In the medium- and high-dose HSYA groups, BFVV was significantly higher than that in the model group ($P < 0.01$), and BFVA was also significantly higher in the high-dose group ($P < 0.01$). This suggests that HSYA reverses the decreased microcirculatory blood flow velocity in the MAFLD model in a dose-dependent manner and improves the microvascular perfusion function.

Table 2. Effects of HSYA on BFVA and BFVV in the mesenteric microvessels of MAFLD rats

Groups	BFVA (mm/s)	BFVV (mm/s)
CON	2.39±0.16	1.41±0.12
MOD	1.84±0.14**	0.89±0.07**
PC	2.33±0.11$^{\#\#}$	1.33±0.09$^{\#\#}$
HSYA-L	1.97±0.20	0.99±0.08
HSYA-M	2.07±0.20	1.11±0.07$^{\#\#}$
HSYA-H	2.20±0.22$^{\#\#}$	1.30±0.06$^{\#\#}$

Note: Data are expressed as mean ± SD (n = 6). $^{**}P < 0.01$ vs. Blank Control group; $^{\#}P < 0.05$, $^{\#\#}P < 0.01$ vs. Model group.

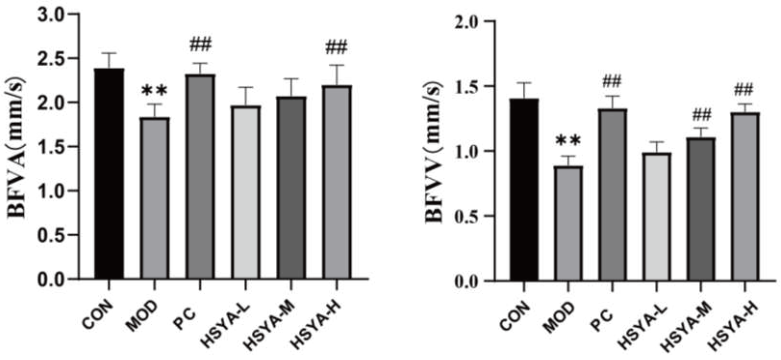


Figure 7. Effects of HSYA on mesenteric microvascular hemodynamics in rats with MAFLD. BFVA (left) and BFVV (right) were measured in the mesenteric microvessels of rats in different groups. Data are presented as mean ± SD (n = 6).$^{**}P < 0.01$ vs. Blank Control group; $^{\#}P < 0.05$, $^{\#\#}P < 0.01$ vs. Model group.

3.5.Effects of HSYA on the EGFR/MAPK/VEGF signaling pathway in MAFLD rats

RT-qPCR results (Figure 8) demonstrated that the mRNA expression levels of EGFR, MAPK1, and VEGF in the livers of the MAFLD model group were significantly upregulated compared with those in the control group. Conversely, HSYA treatment dose-dependently downregulated the expression of these genes compared with the model group, with statistically significant differences obser ved in the high-dose HSYA group. These findings suggest that HSYA may exe rt protective effects by inhibiting overactivation of the EGFR/MAPK/VEGF sig naling pathway.

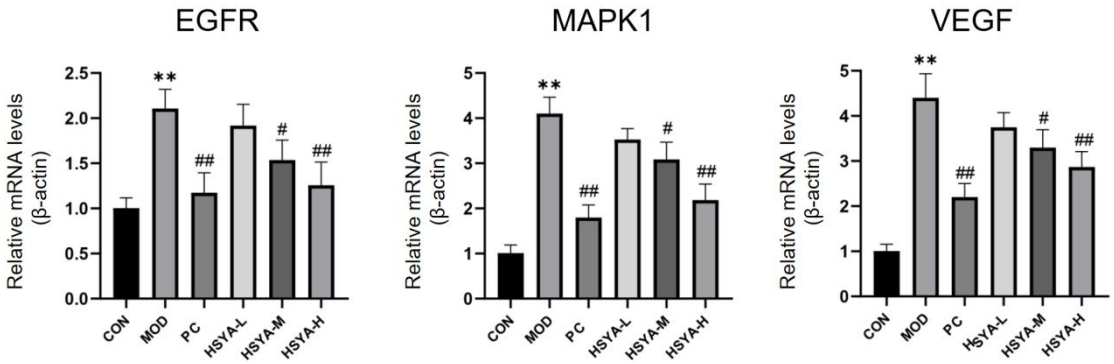


Figure 8. Relative Effects of HSYA on the mRNA expression of EGFR, MAPK1, and VE GF in the liver of MAFLD model rats, determined by RT-qPCR. Data are presented as m ean ± SD (n = 6).$^{**}P < 0.01$ vs. Blank Control group; $^{\#}P < 0.05$, $^{\#\#}P < 0.01$ vs. Model group.

3.6.Effects of HSYA on the protein expression of the EGFR/MAPK/VEGF s ignaling pathway in MAFLD rats

Western blotting results (Figure 9) demonstrated that, compared with the bla nk control group, the ratios of p-EGFR/EGFR and p-MAPK1/MAPK1 in the li ver tissue of the MAFLD model group were significantly increased (P < 0.01), and the protein expression level of VEGF was significantly upregulated (P <

0.01). These findings suggest that the EGFR/MAPK1 signaling pathway is abn ormally activated, inducing pathological angiogenesis.After 4 weeks of interventi on, compared with the model group, the p-EGFR/EGFR and p-MAPK1/MAPK1 ratios decreased in all HSYA treatment groups, with the high-dose group sho wing the most significant improvement ($P < 0.01$). Concurrently, the protein ex pression level of VEGF was significantly downregulated ($P < 0.01$), and the p ositive control group exhibited a similar trend. These results demonstrate that HSYA inhibits EGFR phosphorylation and its downstream MAPK1 signaling an d reduces the abnormal expression of VEGF. This suggests that HSYA amelior ates pathological angiogenesis in MAFLD by inhibiting the EGFR/MAPK1 sign aling pathway.

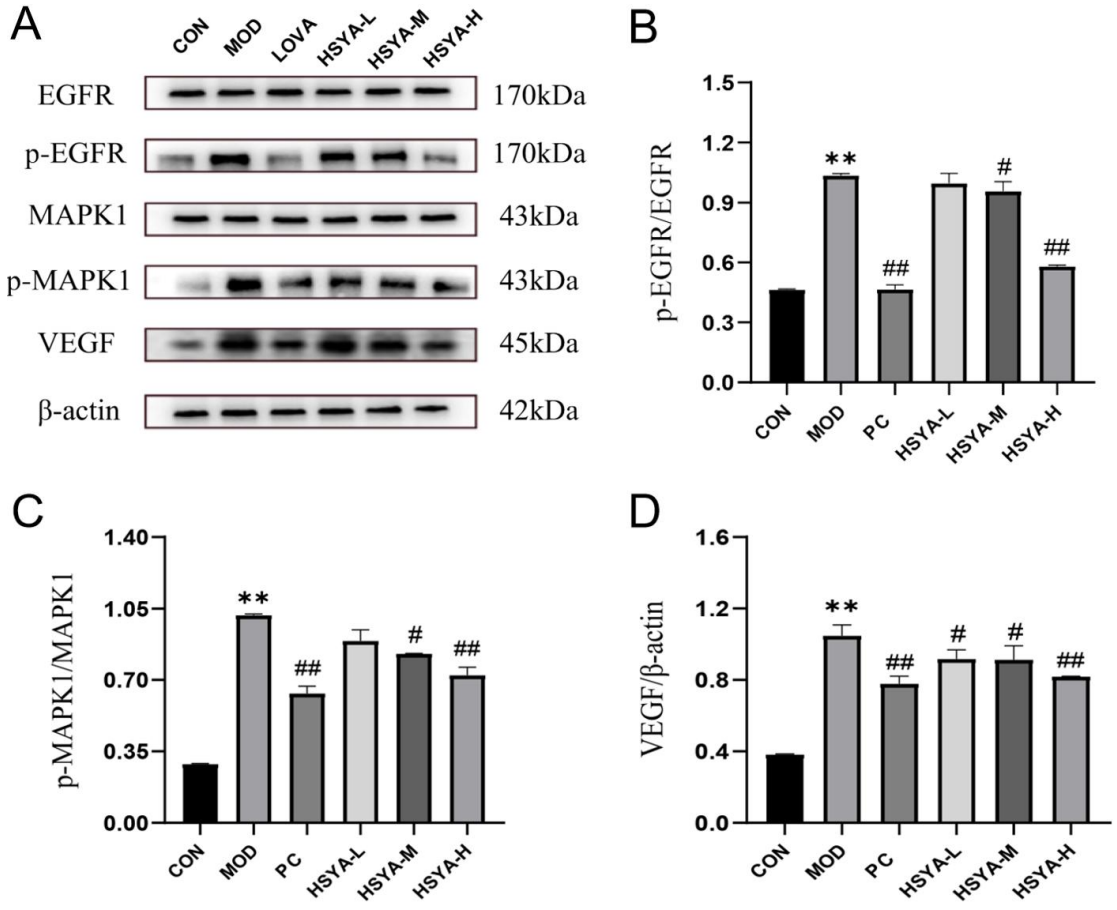


Figure 9. Effects of HSYA on the protein expression of EGFR/MAPK/VEGF signaling pat hway in MAFLD rats.(A) Representative Western blot bands of EGFR, p-EGFR, MAPK1 (ERK2), p-MAPK1, VEGF and β-actin (loading control).(B) Quantitative analysis of p-EGF R/EGFR ratio.(C) Quantitative analysis of p-MAPK1/MAPK1 ratio.(D) Quantitative analysis of VEGF protein expression. Data are presented as mean ± SD ($n = 6$).**$P < 0.01$ vs. Blank Control group; #$P < 0.05$, ##$P < 0.01$ vs. Model group.

3.7.HSYA reduces pathological VEGF expression as revealed by immunohist ochemistry

The results shown in Figure 10(A) demonstrate that VEGF expression was

weak in the liver tissue of the blank control group, with sparse cytoplasmic distribution. In contrast, the MAFLD model group exhibited intense brown-yellow positive staining, indicating a significant upregulation of VEGF expression. Compared with the model group, immunohistochemical staining was markedly attenuated in all treatment groups, with decreased positive staining area and intensity; the positive control and high-dose HSYA groups showed the most pronounced reductions.Semi-quantitative analysis of the mean optical density (MOD), as presented in Figure 10(B), revealed that the VEGF expression level in the model group was significantly higher than that in the blank control group. After a four-week intervention period, the expression levels of VEGF in the positive control group were significantly decreased compared to those in the model group, nearing the levels observed in the blank control group. In the medium- and high-dose HSYA groups, the expression of VEGF was significantly reduced compared to that in the model group . A notable reduction was also evident in the low-dose HSYA group. These results suggest that HSYA effectively suppresses the pathological expression of VEGF in the liver of rats.

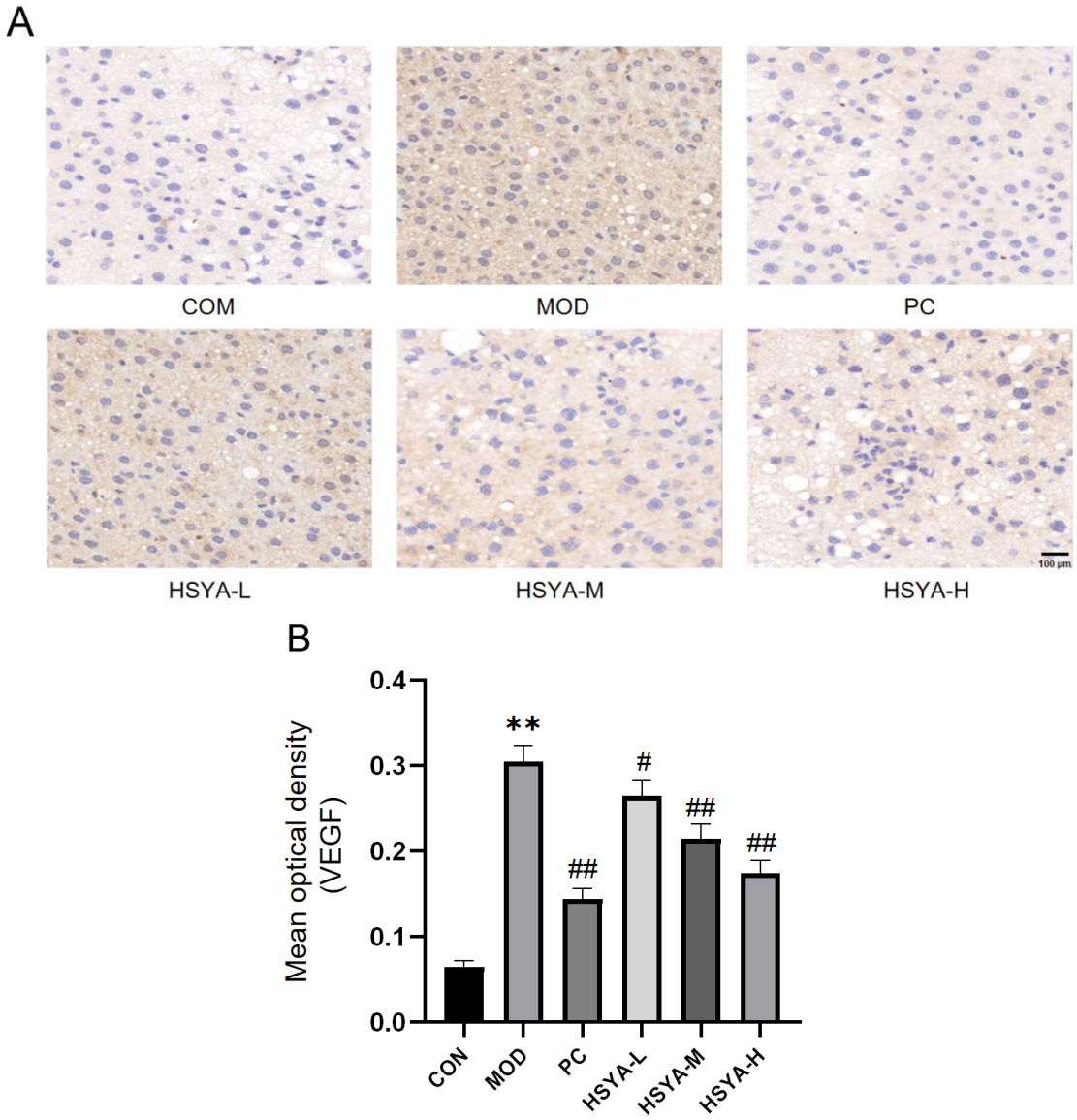


Figure 10. HSYA reduces pathological VEGF expression in the liver of MAFLD model rats detected by immunohistochemistry.(A)Representative photomicrographs of VEGF immunohistochemical staining in liver tissue from each group (×100).(B)Semi-quantitative analysis of mean optical density (MOD) of VEGF expression. Data are presented as mean ± SD (n = 6).**P < 0.01 vs. Blank Control group; #P < 0.05, ##P < 0.01 vs. Model group.

4.Discussion

MAFLD has become a leading cause of chronic liver disease worldwide; however, effective interventions targeting MAFLD-associated microcirculatory dysfunction remain limited. In this study, we provide the first evidence that HSYA, a bioactive chalcone glycoside derived from Carthamus tinctorius L., significantly ameliorated liver injury, lipid metabolism disorders, and microcirculatory disturbances in a MCD diet-induced MAFLD rat model. Our results demonstrated that HSYA not only improved serum transaminase and lipid profiles but also restored mesenteric microvascular morphology and perfusion in rats. Mechanistically, HSYA suppressed aberrant activation of the EGFR/MAPK1 signaling pathway and downregulated VEGF expression, thereby alleviating pathological angiogenesis and endothelial dysfunction. These findings highlight the therapeutic potential of HSYA in MAFLD-associated microcirculatory disorders and elucidate a previously unrecognized mechanism involving the EGFR/MAPK1/VEGF axis.

Hepatic microcirculatory dysfunction is a critical driver of MAFLD progression. In a healthy state, LSECs are characterized by open fenestrae that span the cytoplasm and the absence of a structured basement membrane, forming a discontinuous "fenestrated" endothelium. This unique architecture ensures efficient substrate exchange between plasma components and hepatocytes[22].LSECs are critical regulators of the hepatic microenvironment, maintaining liver homeostasis by modulating vascular tone, inflammatory responses, and thrombogenesis[23].During the early stages of MAFLD, lipotoxicity, oxidative stress, and insulin resistance trigger the "capillarization" of LSECs, characterized by the loss of fenestrae and formation of a structured basement membrane. This phenotypic transition disrupts endothelial barrier function, thereby precipitating microcirculatory dysfunction, exacerbating inflammatory responses, and accelerating the progression of liver fibrosis[24][25].Microvascular structural and functional impairments persist throughout the entire progression. The early stage is primarily characterized by phenotypic alterations in LSECs and narrowing of the hepatic sinusoidal lumen, whereas the late stage is marked by pathological angiogenesis and abnormal vascular remodeling[26].Previous studies employing intravital microscopy have demonstrated that hepatic steatosis results in hepatocyte swelling due to lipid droplet accumulation, which exerts mechanical compression on hepatic sinusoids. Compared with healthy livers, fatty livers exhibit a significant reduction in the number of effectively perfused sinusoids, with a decrease in the sinu

soidal space area of approximately 50%. This mechanical obstruction leads to increased intrahepatic vascular resistance, resulting in a substantial reduction in effective hepatic blood flow[27].The reduction in blood perfusion not only restricts the delivery of oxygen and nutrients but also exacerbates local ischemia and hypoxia, which in turn strongly activates the HIF-VEGF axis. Consequently, this drives abnormal angiogenesis, characterized by highly permeable, structurally immature vessels and unstable compensatory blood flow, ultimately failing to restore microcirculatory homeostasis[28].An imbalance in endothelium-dependent vasomotor function represents the core functional mechanism of microcirculatory dysfunction in MAFLD, where the disruption of the dynamic equilibrium between NO and ET-1 serves as a critical event[29].In the context of insulin resistance, the activity of eNOS is inhibited, resulting in reduced synthesis of NO and compromised endothelium-dependent vasodilation[30]. Simultaneously, diverse inflammatory and hypoxic signals trigger the overexpression of ET-1 in both endothelial cells and hepatic stellate cells, thereby inducing vasoconstriction and increasing intrahepatic vascular resistance[31].In conclusion, the pathogenesis of microcirculatory dysfunction associated with MAFLD is characterized by a complex interaction of several overlapping factors: structural impediments due to the "capillarization" of LSECs, mechanical compression of hepatic sinusoids by steatotic hepatocytes, blood flow turbulence and shunting caused by pathological angiogenesis, and endothelial dysfunction resulting from the imbalance between NO and ET-1. These interconnected mechanisms collectively drive MAFLD disease progression.In our study, an 8-week MCD diet successfully induced profound hepatic steatosis, inflammatory infiltration and microvascular abnormalities. These pathological changes were characterized by a decreased mesenteric DA, increased DV, reduced DA/DV ratio, and significant declines in BFVA and BFVV.Post-HSYA intervention, mesenteric microvascular morphology was notably improved, characterized by an increased DA and an elevated DA/DV ratio. Moreover, the velocity of blood flow increased, and the flow pattern transitioned from a granular to a linear configuration. These findings indicate that HSYA significantly ameliorates microcirculatory perfusion deficits in rats with MAFLD.HSYA intervention significantly increased serum NO levels and decreased ET-1 levels, indicating a substantial restoration of endothelium-dependent vasomotor function.Accumulating evidence suggests that HSYA exerts protective effects on vascular endothelial cells by attenuating inflammatory responses and oxidative stress, thereby preserving their structural integrity. Furthermore, HSYA facilitates the production of endothelium-derived relaxing factors and suppresses the expression of vasoconstrictive factors, acting synergistically to improve microvascular structural and functional remodeling[32]. Moreover, in various metabolism-associated injury models, HSYA has been shown to reduce endothelial hyperpermeability, inhibit apoptosis, and downregulate the expression of adhesion molecules, such as VCAM-1 and ICAM-1, thereby mitigating endothelial inflammatory responses. The current findings provide further evidence supporting the therapeutic efficacy of HSYA in ameliorating microcirculatory dysfunction associated

with MAFLD[33].We acknowledge that the ideal endpoint for this study would be direct assessment of hepatic sinusoidal microcirculation (e.g., by intravital microscopy of the liver). However, technical challenges, including respiratory motion artifacts, tissue photodamage, and the fragility of MCD diet-induced livers, precluded stable intravital imaging in our experimental setting. As an alternative, we examined mesenteric microvessels, which are widely used in microcirculation research as a stable and reproducible model of systemic/peripheral microcirculation. We recognize that this substitution introduces key limitations: MAFLD is associated with generalized endothelial dysfunction, but the mesenteric microcirculation cannot assess liver-specific structural changes, such as sinusoidal capillarization or loss of LSEC fenestration. Although our results showed that HSYA-induced improvements in mesenteric parameters correlated well with reductions in liver injury, inflammation, and the EGFR/MAPK1/VEGF pathway, our conclusions regarding microcirculatory improvement are strictly limited to the mesenteric bed. Additional studies using direct hepatic imaging are required to confirm whether HSYA similarly improves hepatic sinusoidal perfusion.

EGFR is a member of the receptor tyrosine kinase family. Upon activation via phosphorylation, it triggers the downstream RAS-RAF-MEK-ERK signaling cascade, a pathway extensively involved in the regulation of genes associated with cell proliferation, inflammatory responses and angiogenesis[34].MAPK1 (ERK2), a critical downstream effector of this pathway, transduces extracellular signals into the nucleus upon phosphorylation, thereby modulating processes such as hepatic lipid metabolic disorders and vascular remodeling[35]. Evidence has demonstrated that the EGFR/MAPK1 signaling axis is a pivotal mediator of MAFLD progression. Under conditions of metabolic stress, characterized by hepatic steatosis and an inflammatory milieu, free FFAs and pro-inflammatory cytokines can induce aberrant phosphorylation of EGFR, subsequently triggering the downstream MAPK1 signaling cascade[36].Both RT-qPCR and Western blot results in this study consistently demonstrated elevated expression and phosphorylation levels of EGFR and MAPK1 in the MCD-induced model, indicating the constitutive activation of this signaling axis. Notably, HSYA treatment significantly attenuated the p-EGFR/EGFR and p-MAPK1/MAPK1 ratios. These findings suggest that the beneficial effects of HSYA on microcirculatory perfusion are, at least in part, mediated by the inhibition of EGFR/MAPK1-driven pathological angiogenesis.Furthermore, HSYA suppresses HSC activation and pathological angiogenesis in liver fibrosis models. By modulating the miR-29a-3p/PDGFRB axis, HSYA blocks PDGFRB/MEK/ERK signaling transduction, subsequently downregulating the expression of HIF-1α, VEGFA, and VEGFR2. This effectively ameliorates fibrosis and pathological vascular remodeling[37]. These findings provide additional mechanistic support for the role of HSYA in regulating ERK-associated pathways, intervening in abnormal angiogenesis, and improving the hepatic microenvironment and microcirculatory dysfunction.

VEGF is a core mediator of angiogenesis, vascular permeability, and endothelial cell function, playing a pivotal role in vascular remodeling and maintena

nce of microvascular homeostasis[38]. Under pathological conditions, such as st eatosis, local tissue hypoxia, and inflammatory stimuli, VEGF expression is abe rrantly upregulated[39]. This overexpression facilitates pathological angiogenesis, leading to disrupted vascular architecture, functional impairment, and reduced blood perfusion, which collectively exacerbate microcirculatory perfusion deficits. The results of this study consistently demonstrated that both mRNA and protei n expression levels of VEGF were significantly upregulated in the liver tissues of the MAFLD model group. Immunohistochemical analysis corroborated these findings, showing a marked increase in VEGF-positive staining in the model group. Taken together with the hemodynamic assessments, these findings sugges t that aberrant VEGF expression may actively contribute to structural remodelin g and impairment of microcirculatory perfusion in MAFLD livers.Research has indicated that hypoxia-inducible factor-1α (HIF-1α) acts as a critical transcriptio nal activator of VEGF[40]. In MAFLD, hepatic steatosis induces local tissue h ypoxia, which triggers VEGF expression. Furthermore, the EGFR/MAPK1 signa ling pathway plays a pivotal role in the regulation of angiogenesis[41]. Phosph orylated MAPK1 can indirectly up-regulate VEGF expression by enhancing the protein stability and transcriptional activity of HIF-1α.Existing studies have de monstrated that cancer cells harboring activated EGFR can release microvesicles to transfer oncogenic signals to endothelial cells. This process facilitates the a ctivation of the MAPK pathway within endothelial cells, subsequently inducing the autocrine expression of VEGF and driving pathological angiogenesis[42].In this study, the concurrent elevation of EGFR and MAPK1 phosphorylation lev els alongside significantly upregulated VEGF expression in the model group su ggests a strong correlation and potential causal relationship between the aberran t activation of the EGFR/MAPK1 axis and VEGF upregulation in the progressi on of MAFLD. Notably, HSYA intervention reduced the activation of both EG FR and MAPK1 in a dose-dependent manner, accompanied by a corresponding downregulation of VEGF. This consistent trend indicates that HSYA modulates VEGF-mediated angiogenesis while inhibiting the EGFR/MAPK1 signaling pat hway in HUVECs. Combined with the observed improvements in microcirculat ory hemodynamics, these findings suggest that HSYA restores pathological vasc ular structures and improves microcirculatory perfusion by inhibiting the EGFR/ MAPK1 signaling axis and subsequently modulating the aberrant expression of VEGF.

Conclusion

In summary, our study demonstrates that rats with MAFLD exhibit severe hepatic impairment, dyslipidemia, and microcirculatory dysfunction, which are a ccompanied by the aberrant activation of the EGFR/MAPK1 signaling axis and the up-regulation of the pro-angiogenic factor VEGF. HSYA intervention signif icantly improved metabolic profiles, restored endothelium-dependent vasomotor f unction, and normalized mesenteric microvascular hemodynamics. Furthermore, HSYA treatment effectively suppressed the phosphorylation of EGFR and MAP

K1 and down-regulated VEGF expression at both transcriptional and translation al levels. Collectively, these findings indicate that HSYA exerts its therapeutic effect on MAFLD-associated microcirculatory impairment by targeting the EGF R/MAPK1 signaling pathway to modulate VEGF-mediated pathological angiogen esis. These results provide robust experimental evidence supporting the potential clinical application of HSYA in the management of MAFLD.

Author Contributions: Qing Liu: Conceptualization, Investigation, Writing-origi nal draft, Visualization. Nan Ai: Investigation, Formal analysis, Writing-review& editing. Rui Wang: Methodology, Resources, Writing-review&editing. Zhenbo Li: Software, Formal analysis, Data curation. Yihan Liu: Investigation, Validatio n. Lei Wu: Resources, Writing-review&editing. Yuqin Zhao: Methodology, Supe rvision. Jing Yang: Conceptualization, Funding acquisition, Project administratio n, Supervision, Writing-review&editing.

Acknowledgements: This study is supported by Central Government Supports L ocal College Reform Projects and National Natural Science Foundation of Chin a, Heilongjiang Touyan Innovation Team Program.The authors thank Dr.Wang a nd Dr. Yang for their technical and clerical assistance.

Funding: Central Government Supports Local College Reform Projects(8160341 8)；Heilongjiang Touyan Innovation Team Program(2020YQ05)

Ethics Statement: The animal study protocol was approved by the Laboratory Animal Ethics Committee of Heilongjiang University of Chinese Medicine (App roval No.SCXK(Liao)2020-0001). All experiments were conducted in full compl iance with the Guide for the Care and Use of Laboratory Animals published b y the US National Research Council and reported in accordance with the ARR IVE guidelines.Clinical trial number: not applicable.

Consent: All patients in this trial provided written informed consent.

Data Availability: The data that support the findings of this study are availabl e on request from the corresponding author. The data are not publicly available due to privacy or ethical restrictions.

References

[1] Li C, Yu S, Li X, et al. Medicinal formula huazhi-rougan attenuates non-alcoholic ste atohepatitis through enhancing fecal bile acid excretion in mice[J]. Frontiers in Pharm acology, 2022, 13: 833414.

[2] Eslam M, Fan JG, Yu ML, Wong VW, Cua IH, Liu CJ,et al. The Asian Pacific asso ciation for the study of the liver clinical practice guidelines for the diagnosis and ma nagement of metabolic dysfunction-associated fatty liver disease. Hepatol Int. 2025 Ap r;19(2):261-301.

[3] Hou M M, Gu Q, Cui J W, et al. Proportion and clinical characteristics of metabolic -associated fatty liver disease and associated liver fibrosis in an urban Chinese popula tion[J]. Chinese Medical Journal, 2025, 138(7): 829-837.
[4] Bo T, Gao L, Yao Z, Shao S, Wang X, Proud CG, Zhao J. Hepatic selective insulin resistance at the intersection of insulin signaling and metabolic dysfunction-associated steatotic liver disease. Cell Metab. 2024 May 7;36(5):947-968.
[5] Huby T, Gautier EL. Immune cell-mediated features of non-alcoholic steatohepatitis. N at Rev Immunol. 2022 Jul;22(7):429-443.
[6] Song C, Long X, He J, Huang Y. Recent evaluation about inflammatory mechanisms in nonalcoholic fatty liver disease. Front Pharmacol. 2023 Mar 16;14:1081334.
[7] Clare K, Dillon JF, Brennan PN. Reactive Oxygen Species and Oxidative Stress in th e Pathogenesis of MAFLD. J Clin Transl Hepatol. 2022 Oct 28;10(5):939-946.
[8] Xu J, Chen N, Li Z, Liu YL. Gut microbiome and liver diseases. Fundam Res. 2025; 5(2):890-901.
[9] Gracia-Sancho J, Marrone G, Fernández-Iglesias A. Hepatic microcirculation and mech anisms of portal hypertension. Nat Rev Gastroenterol Hepatol. 2019 Apr;16(4):221-23 4.
[10] Hammoutene A, Rautou PE. Role of liver sinusoidal endothelial cells in non-alcoholic fatty liver disease. J Hepatol. 2019 Jun;70(6):1278-1291.
[11] Wree A, Holtmann TM, Inzaugarat ME, Feldstein AE. Novel Drivers of the Inflamma tory Response in Liver Injury and Fibrosis. Semin Liver Dis. 2019 Jul;39(3):275-282.
[12] Gracia-Sancho J, Caparrós E, Fernández-Iglesias A, Francés R. Role of liver sinusoida l endothelial cells in liver diseases. Nat Rev Gastroenterol Hepatol. 2021 Jun;18(6):41 1-431.
[13] Yan M, Cui Y, Xiang Q. Metabolism of hepatic stellate cells in chronic liver diseases: emerging molecular and therapeutic interventions. Theranostics. 2025 Jan 2;15(5):1715 -1740.
[14] Liu X, Tan S, Liu H, Jiang J, Wang X, Li L, Wu B. Hepatocyte-derived MASP1-enr iched small extracellular vesicles activate HSCs to promote liver fibrosis. Hepatology. 2023 Apr 1;77(4):1181-1197.
[15] Wang C, Ma C, Gong L, Guo Y, Fu K, Zhang Y, Zhou H, Li Y. Macrophage Polari zation and Its Role in Liver Disease. Front Immunol. 2021 Dec 14;12:803037.
[16] Du W, Wang L. The Crosstalk Between Liver Sinusoidal Endothelial Cells and Hepati c Microenvironment in NASH Related Liver Fibrosis. Front Immunol. 2022 Jun 28;13: 936196.
[17] Liu P, Liang WL, Huang RT, Chen XX, Zou DH, Kurihara H, Li YF, Xu YH, Ouya ng SH, He RR. Hepatic microcirculatory disturbance in liver diseases: intervention wit h traditional Chinese medicine. Front Pharmacol. 2024 Jul 23;15:1399598.
[18] Ai N, Wang XC, Liu XY, Liu Q, Wang R, Yang J. Research progress on hepatoprote ctive effects of hydroxysafflor yellow A. Drugs & Clinic. 2025;40(1):229-233.
[19] Liu Y, Xu W, Zhai T, You J, Chen Y. Silibinin ameliorates hepatic lipid accumulation and oxidative stress in mice with non-alcoholic steatohepatitis by regulating CFLAR-JNK pathway. Acta Pharm Sin B. 2019 Jul;9(4):745-757.
[20] Yang L, Liu Q, Zhang H, et al. Silibinin improves nonalcoholic fatty liver by regulat

ing the expression of miR-122: an in vitro and in vivo study[J]. Molecular Medicine Reports, 2021, 23(5): 335.

[21] Li Y, Shi Y, Sun Y, Liu L, Bai X, Wang D, Li H. Restorative effects of hydroxysaff lor yellow A on hepatic function in an experimental regression model of hepatic fibro sis induced by carbon tetrachloride. Mol Med Rep. 2017 Jan;15(1):47-56.

[22] Qu J, Wang L, Li Y, Li X. Liver sinusoidal endothelial cell: An important yet often overlooked player in the liver fibrosis. Clin Mol Hepatol. 2024 Jul;30(3):303-325.

[23] Poisson J, Lemoinne S, Boulanger C, Durand F, Moreau R, Valla D, Rautou PE. Liv er sinusoidal endothelial cells: Physiology and role in liver diseases. J Hepatol. 2017 Jan;66(1):212-227.

[24] Gracia-Sancho J, Caparrós E, Fernández-Iglesias A, Francés R. The role of liver sinus oidal endothelial cells in liver diseases: Key players in health and pathology. Journal of Hepatology. 2026;84(3):655-672.

[25] Dai Q, Ain Q, Seth N, Rooney M, Zipprich A. Liver sinusoidal endothelial cells: Fri end or foe in metabolic dysfunction- associated steatotic liver disease/metabolic dysfun ction-associated steatohepatitis. Dig Liver Dis. 2025 May;57(5):493-503.

[26] Hirayama AB, Taliberti IB, Oliveira CPMS, Alves VAF. LIPOTOXICITY PLAYS A KEY ROLE IN THE DEVELOPMENT OF ANGIOGENESIS AND MICROCIRCULA TORY MODULATION IN MASLD SPECTRUM. Arq Gastroenterol. 2025 Oct 27;62: e25053.

[27] Farrell GC, Teoh NC, McCuskey RS. Hepatic microcirculation in fatty liver disease. Anat Rec (Hoboken). 2008 Jun;291(6):684-92.

[28] Carmeliet P, Jain RK. Molecular mechanisms and clinical applications of angiogenesis. Nature. 2011 May 19;473(7347):298-307.

[29] Bosch J, Abraldes JG, Fernández M, García-Pagán JC. Hepatic endothelial dysfunction and abnormal angiogenesis: new targets in the treatment of portal hypertension. J He patol. 2010 Sep;53(3):558-67.

[30] Pasarín M, Abraldes JG, Liguori E, Kok B, La Mura V. Intrahepatic vascular changes in non-alcoholic fatty liver disease: Potential role of insulin-resistance and endothelial dysfunction. World J Gastroenterol. 2017 Oct 7;23(37):6777-6787.

[31] Degertekin B, Ozenirler S, Elbeg S, Akyol G. The serum endothelin-1 level in steatos is and NASH, and its relation with severity of liver fibrosis. Dig Dis Sci. 2007 Oct;5 2(10):2622-8.

[32] Wang Y, An J, Zhou J, Chang L, Zhang Q, Peng F. Hydroxysafflor yellow A: a natu ral pigment with potential anticancer therapeutic effect. Front Pharmacol. 2025 Jan 14; 15:1495393.

[33] Zhang X, Shen D, Feng Y, Li Y, Liao H. Pharmacological Actions, Molecular Mecha nisms, Pharmacokinetic Progressions, and Clinical Applications of Hydroxysafflor Yello w A in Antidiabetic Research. J Immunol Res. 2021 Dec 13;2021:4560012.

[34] Choung S, Kim JM, Joung KH, Lee ES, Kim HJ, Ku BJ. Epidermal growth factor re ceptor inhibition attenuates non-alcoholic fatty liver disease in diet-induced obese mice. PLoS One. 2019 Feb 8;14(2):e0210828.

[35] Martin-Vega A, Cobb MH. ERK1/2-MAPK signaling: Metabolic, organellar, and cytos keletal interactions. Curr Opin Cell Biol. 2025 Aug;95:102526.

[36] Tito C, Masciarelli S, Colotti G, Fazi F. EGF receptor in organ development, tissue h omeostasis and regeneration. J Biomed Sci. 2025 Feb 19;32(1):24.

[37] Xue X, Li Y, Zhang S, Yao Y, Peng C, Li Y. Hydroxysafflor yellow A exerts anti-fi brotic and anti-angiogenic effects through miR-29a-3p/PDGFRB axis in liver fibrosis. Phytomedicine. 2024 Sep;132:155830.

[38] Koperska A, Miller-Kasprzak E, Seraszek-Jaros A, Musialik K, Bogdański P, Szulińsk a M. The Influence of Berberine on Vascular Function Parameters, Among Them VE GF, in Individuals with MAFLD: A Double-Blind, Randomized, Placebo-Controlled Tri al. Nutrients. 2025 Nov 16;17(22):3585.

[39] Hirayama AB, Taliberti IB, Oliveira CPMS, Alves VAF. LIPOTOXICITY PLAYS A KEY ROLE IN THE DEVELOPMENT OF ANGIOGENESIS AND MICROCIRCULA TORY MODULATION IN MASLD SPECTRUM. Arq Gastroenterol. 2025 Oct 27;62: e25053.

[40] Redaelli CA, Semela D, Carrick FE, Ledermann M, Candinas D, Sauter B, Dufour JF. Effect of vascular endothelial growth factor on functional recovery after hepatectomy in lean and obese mice. J Hepatol. 2004 Feb;40(2):305-12.

[41] Han L, Lin X, Yan Q, Gu C, Li M, Pan L, Meng Y, Zhao X, Liu S, Li A. PBLD i nhibits angiogenesis via impeding VEGF/VEGFR2-mediated microenvironmental cross-t alk between HCC cells and endothelial cells. Oncogene. 2022 Mar;41(13):1851-1865.

[42] Al-Nedawi K, Meehan B, Kerbel RS, Allison AC, Rak J. Endothelial expression of a utocrine VEGF upon the uptake of tumor-derived microvesicles containing oncogenic EGFR. Proc Natl Acad Sci U S A. 2009 Mar 10;106(10):3794-9.

Supplementary Files

This is a list of supplementary files associated with this preprint. Click to download.

- wb.zip